A Virtual Synchronous Machine Implementation and a Tuning Strategy for its Excitation and Governing Systems

Sabrina de Angeli Souza
Lucas F. Encarnação
Daniel Carletti
Federal University of Espírito Santo
Vitória, Espírito Santo, Brazil

Marcelo Brunoro
Federal Institute of Espírito Santo
Vitória, Espírito Santo, Brazil

***Abstract*—The Virtual Synchronous Generator (VSG) consists in a control strategy to make a converter interface between a Distributed Generation unit and the grid operate as a Synchronous Machine. The diffusing utilization of distributed generation units has changed the traditional structure of the power system that is dominated by synchronous machines and centralized power plants. Hence, as these sources have small rotating mass and are poorly damped, the VSG is a solution to improve power grid transient stability.**

This paper is focused on a VSG implementation and its controller tuning in order to guarantee a proper time domain response. A control design methodology is proposed separately for the voltage and speed controllers based on the location of the system eigenvalues. Finally, to validate the VSG model, its simulations results are compared with the results from an equivalent synchronous generator when the grid is subjected to a few disturbances.

***Index Terms*-- Distributed Generation, Grid Stability, Inertia Emulation, Power Electronic Converters, Virtual Synchronous Generator.**

I. INTRODUCTION

In large centralized power stations, the interconnected synchronous generators and its rotating mass turn the grid into an infinite busbar, whose parameters like voltage, frequency and phase sequence remain constant even during a major fault or in response to a disturbance. However, the installed capacity of distributed generators and microgrids in the power system is growing, changing the traditional structure dominated by centralized power plants.

Distributed generation units (DG) include renewable energy technologies that are dependent on geological location, such as wind turbines, geothermal energy production, solar systems (photovoltaic and combustion) and some hydro-thermal plants. The mainly disadvantage regarding these sources is their very small or no rotating mass and poor damping property. Furthermore, most of these DG units only consider supplying maximum power to the grid without taking the stability of the power system in account.

As an effect of the low inertia and damping proprieties of DG units, the corresponding transient stability is reduced, so that the grid is no longer able to withstand large disturbances such as short circuits, loss of a generation, changing of a load demand or even loss of a portion of transmission network. The operation of few small-size DG units can not affect the operation of the nearby grid connected to a large centralized power system, but a significant number of DG with higher capacities can impact the overall dynamic of power system.

A proposed solution already discussed in references [1]-[3] is to control the power electronics inverter/converter operation to emulate the synchronous machine behavior. This concept is known as Virtual Synchronous Generator (VSG), which consist in a control mechanism through which the DG can reproduce the static and dynamic characteristics of a real synchronous machine on a power electronic interface.

This paper presents a VSG implementation as well as its control mechanism, including a methodology for controller tuning and stability improvement by means of the system eigenvalues location with respect to the controllers parameters. Models for all VSG elements are detailed in order to exhibit the relation of the voltage and speed controllers with the system parameters. Finally, the validity and accuracy of the presented VSG are obtained comparing the results from time-domain simulation of a VSG with an equivalent synchronous machine during some disturbance events.

II. VIRTUAL SYNCHRONOUS MACHINE MODELLING

As the Virtual Synchronous Generator was modeled with the purpose of emulate a Synchronous Machine (SM), the development consider the mathematical equations regarding a SM [4]-[5], which includes a 5^{th} order model for electrical circuit in dq-representation and a 2^{nd} order mechanical model, resulting in a 7^{th} order complete model. Certain simplifications can be applied depending on the degree of complexity and accuracy required [6]. This paper has implemented a 4th order model for which the effects concerning damping windings are neglected and the model is described according to the equations (1) ~ (7):

Mechanical equations:

$$T_m - T_e - D \cdot \Delta\omega = \frac{P_m}{\omega} - \frac{P_e}{\omega} - D \cdot \Delta\omega = J\frac{d\omega}{dt} \qquad (1)$$

$$\frac{d\theta}{dt} = \omega \qquad (2)$$

Where T_m is the mechanical torque; T_e is the electromagnetic torque which is generated from rotating magnetic field; P_e and P_m are corresponding to mechanical and electromagnetic power; D is the rotation friction factor; ω is rotor rotation speed; J is the inertia coefficient; θ is the rotor mechanical angle.

Electrical equations:

$$P_e = E_q' I_q + E_d' I_d + (x_d' - x_q') I_d I_q \qquad (3)$$

$$\tau_{d0}' \cdot \dot{E_q'} = E_f - E_q' + I_d(x_d - x_d') \qquad (4)$$

$$\tau_{q0}' \cdot \dot{E_d'} = -E_d' - I_q(x_q - x_q') \qquad (5)$$

$$V_{td} = E_d' - x_q' \cdot i_q - I_d \cdot r \qquad (6)$$

$$V_{tq} = E_q' + x_d' \cdot i_d - I_q \cdot r \qquad (7)$$

Where τ_{d0}' and τ_{q0}' are dq-axis transient open-circuit time constants; x_d and x_q are dq-axes components of synchronous reactance; x_d' and x_q' are dq-axes components of transient reactance; I_d and I_q are dq-axes components of current; E_d' and E_q' are dq-axes components of transient voltage; E_f is exciter voltage; V_{td} and V_{tq} are dq-axes components of terminal voltage; r is stator windings resistance.

Above equations were applied in the block diagram representation of Fig. 1, where the parameters and transfer functions are detailed in [6]. Notice that Fig.1 includes a speed governor, which is a speed controller, and an excitation system, which corresponds to a controller for terminal voltage. Thus there are two control loops, the first one where the governor controls the flow rate though valves with the objective of maintaining the speed constant, and a second one where the excitation system provides a field voltage to regulate the terminal voltage. In addition, these control loops are highlighted in Fig. 1 and the visible interaction between them is neglected during the control tuning since this cross-coupling is usually weak.

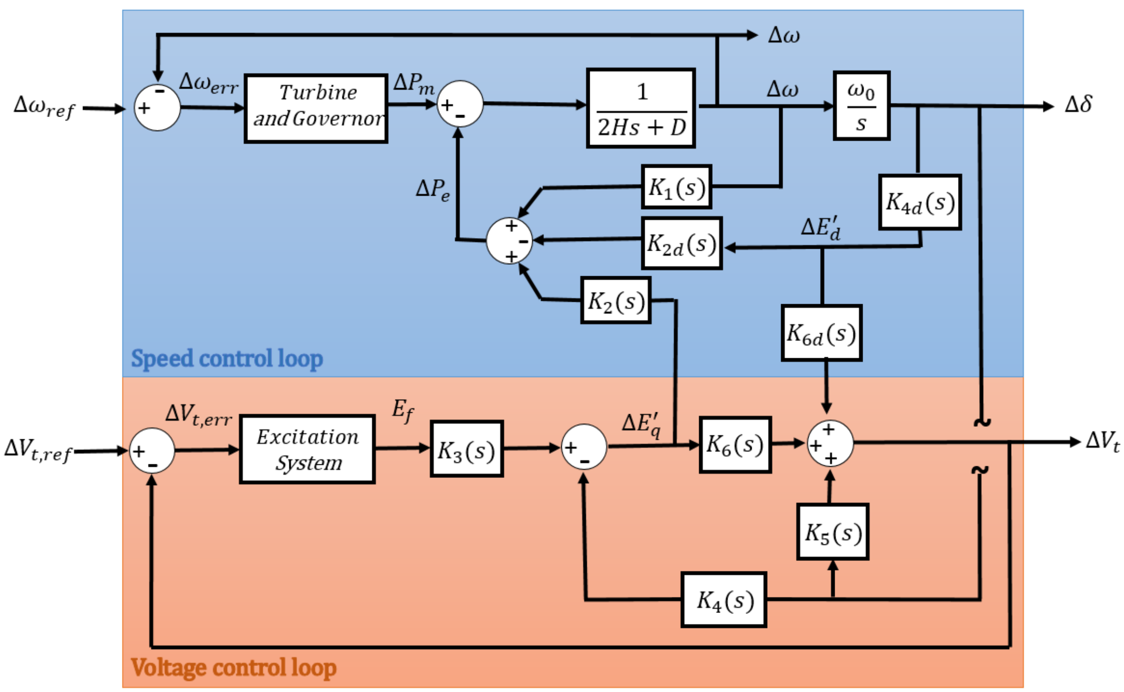

Figure 1. Block diagram of synchronous generator including a governor and an excitation system. Modified from [6] by the author.

III. Control Tuning Methods For Excitation And Governing Systems

Controllers tuning for excitation and governing systems are necessary to meet a desired transient response. Thereby, the controller parameters must be adjusted in order that the response of the closed-loop control systems to incremental changes in system conditions can reach design specifications, such as: Rise time, overshoot, settling time, phase margin and gain margin. Selecting parameters without a proper control design can lead to a slow response and the controller will not be able to handle upsets or reach setpoint in due time; On the other hand, selecting parameters to an aggressive control action can lead the control system to an oscillatory or unstable response.

This paper proposes a methodology for tuning the parameters of speed and voltage controllers in order to guarantee a stable operation and design requirements cited above. The controller design is developed for a synchronous generator and its adjusted parameters can be applied to an equivalent VSG.

A. Governor System Tuning

As the cross–coupling is weak, the design task reduces to a single-input and single-output design for each control loop. The closed loop for speed control is represented in Fig. 2, where the turbine time constants were neglected and the governor transfer function is just a droop control with a 1/Dp gain [4]. H is a constant representative of the machine and it's associated with the inertia coefficient. Notice that this picture is part of Fig.1.

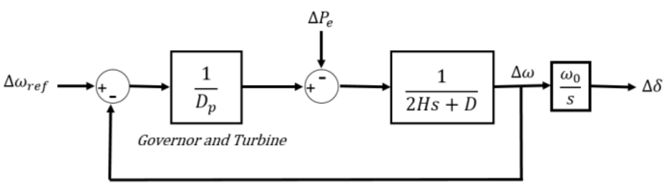

Figure 2. Closed loop block diagram for speed control.

The characteristic equation of the closed-loop system and the resulting time constant are indicated in (8) and (9), respectively.

$$2 \cdot H \cdot s + D + \frac{1}{D_p} = 0 \quad (8)$$

$$\tau_{speed} = \frac{2 \cdot H}{D + \frac{1}{D_p}} \quad (9)$$

For stability, the roots of (8) have to be in the left side of complex s-plane. In this case, the closed-loop is represented by a first order transfer function and a sufficient and necessary condition is that the coefficient $D+1/D_p$ is positive. Consequently, D_p must be positive.

Moreover, as settling time is directly related to the resulting time constant, another constraint must be applied in D_p to achieve the required response time. Thus, if the settling time t_s was established as five times the time constant yields:

$$D_p \approx \frac{t_s}{10 \cdot H - D \cdot t_s} \quad (10)$$

Therefore, the speed controller in this approach is stable whereas Dp>0 and its tuning is summarized to the basic condition in (10).

B. Excitation System Tuning

The closed-loop for voltage control is represented in Fig.3, where the excitation system highlighted in gray is combined with the machine's inner behavior. This block diagram is an adaptation of the DC2A excitation system of the IEEE [7], to which a value for K_E=1 is used to represent a separately excited exciter. In Fig.3, time constant T_A and gain K_A are associated with the voltage regulator; V_R is the voltage regulator output, where $V_{R,Max}$ and $V_{R,Min}$ are its bound limits; T_E and K_E are constants with respect to exciter; T_F and K_F are used to provide a feedback signal for excitation system stabilization.

From Fig.3, the characteristic equation of the closed-loop system and its coefficients C_i are defined in Table I.

$$C_4 s^4 + C_3 s^3 + C_2 s^2 + C_1 s + C_0 = 0 \quad (11)$$

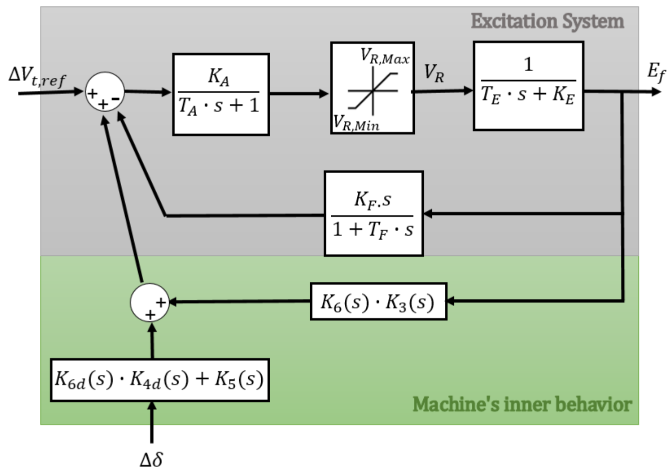

Figure 3. Closed loop block diagram for voltage control.

Note that the closed-loop poles are dependent on tuning parameters of the excitation system T_A, T_F, T_E, K_A and K_F. As the pole location defines the transient and steady state response, the control tuning is focused on pole placement strategy [8]. Hence, the first step is to restrict the root locus region to achieve the design specifications prescribed as overshoot and settling time. Then a set of poles must be selected inside of this region, taking into consideration the characteristic equation order. Finally, the parameters T_A, T_F, T_E, K_A and K_F shall be adjusted in a way that roots in (11) match with the selected poles.

However, due the relationship between the coefficients in (11), it's not possible to choose all the parameters freely. To overcome this problem, an objective function (12) based on least squares method was implemented in order to find the values of T_A, T_F, T_E, K_A and K_F that turn the roots of (11) more closely to the desired poles. When (12) return its minimum value, the set of optimal parameter is found.

$$z = \sum_{i=0}^{4} (P_i - C_i)^2 \quad (12)$$

IV. Simulation Validation And Results Discussion

The simulation was developed in the PSCAD environment and Fig. 4 shows an overview of the schematic applied to the simulated system. The VSG is connected to an infinite bus via a tie-line reactance x_{tl}, which is also connected to a 3-Phase constant load Q_{load}, P_{load}. Additionally, a LCL filter was introduced with the purpose of reducing high-frequency harmonics components generated by the 3ϕ inverter. The filter settings L_1, L_f and C_f were designed according to [9].

TABLE I. COEFFICIENTS OF THE CHARACTERISTIC EQUATION

Order	Coefficients of Characteristic Equation	Desired Coefficients
s^4	$C_4 = T_A T_F T_E \tau'_{d0}(x'_d + x_{tl})$	P_4
s^3	$C_3 = \tau'_{d0}(x'_d + x_{tl})(T_A T_E + T_A T_F + T_F T_E) + (x_d + x_{tl}) T_A T_E T_F$	P_3
s^2	$C_2 = \tau'_{d0}(x'_d + x_{tl})(T_A + T_E + T_F) + (x_d + x_{tl})(T_A T_E + T_A T_F + T_F T_E) + \tau'_{d0}(x'_d + x_{tl}) K_A K_F$	P_2
s^1	$C_1 = (x_d + x_{tl})(T_A + T_E + T_F + K_A K_F) + \tau'_{d0}(x'_d + x_{tl}) + x_{tl} K_A T_F$	P_1
s^0	$C_0 = x_d + x_{tl} + x_{tl} K_A$	P_0

The VSG structure diagram is the same as Fig. 5, where the measurements of voltage and current at the converter interface to the grid feed the VSG, which calculates the voltages that a real SM would produce [10][11]. Simulation parameters are as following: ω_0=2π60; V_n=220V; x_{tl}=0.23; P_{load}=38kW; Q_{load}=15kVAr; L_1=0.6914mH; L_f=0.1521mH; C_f=137.0125µF; P_n=50kW; r=0.008; x_d=1.45; x_q=1.42; x_d'=x_q'=0.28; τ_{d0}'=2.8s; τ_{q0}'=0.001s; J=0.05; D=0; v_{DC}=500V. The parameters of the excitation and governor systems were obtained according to the tuning procedures described in the previous section. They are summarized in Table II.

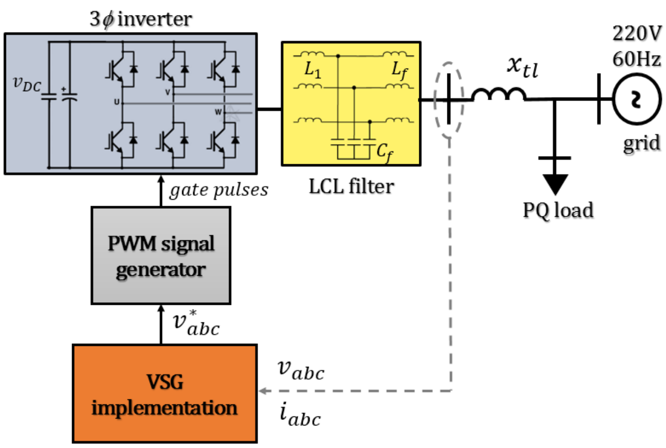

Figure 4. Overview of the functional diagram and the control structure applied for the simulated system

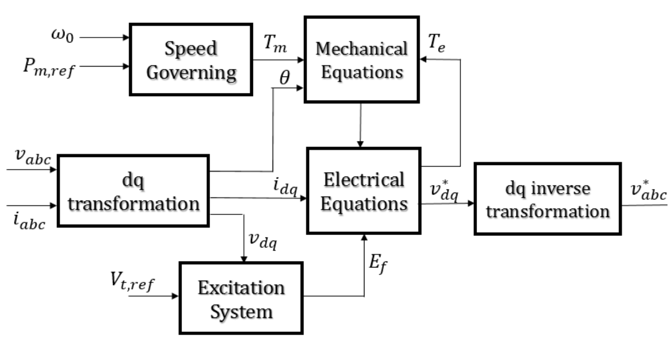

Figure 5. VSG Implementation providing voltage references

TABLE II. EXITATION AND GOVERNING SYSTEM PARAMETERS

D_p	K_a	T_a	K_e	T_e	K_f	T_f	$V_{R,Min}/V_{R,Max}$
0.355	163	0.1	1	0.01	0.0007	0.108	-5.0/5.0

The simulation was started at t=0 and after 2s a voltage sag occurs, reducing the infinite bus voltage to 50% with a duration of 200ms. At 4s of simulation, the active power reference $P_{m,ref}$ changes from 0,6pu to 1pu. Then at t=5s, a three-phase short circuit occurs and lasts 200ms. Fig. 6 to Fig.14 shows the simulation results under these electrical disturbances.

From Fig.6 to Fig.9, it was verified that terminal voltage and reactive power are not affected by D_p, but the settling time becomes smaller as D_p decreases for a change in active power reference. Nevertheless, despite a small D_p makes the system faster, a substantial reduction can lead the system to an oscillatory response, as it's clearly shown for D_p=0.1.

It is worth mentioning that (10) and (11) relies on machine's inner parameters and line reactance, hence if any data is not correctly known, or if it changes because of motor heating or other variations, the result will be the detuning of the controller and the desired transient response may not be reached. To evidence these effects, changes in x_{tl} and τ'_{d0} over 20% are applied and the results are plotted together with the original system in Fig.10, 11, 12 and 13. Besides providing a measure of parametric sensitivity, these detuning gives useful insights for stability analysis and allows evaluating the impacts of selecting parameters without a proper control design.

In Fig 10, 11, 12 and 13, the original parameters provide a faster response as can be seen through rise time and settling time after grid disturbances. When a detuning occur, the VSG

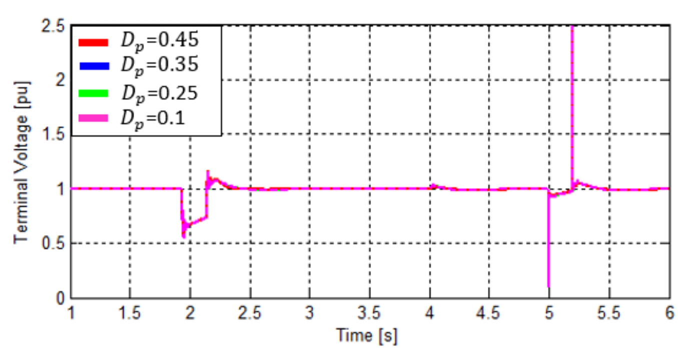

Figure 6. Terminal voltage response for variations in governing system tuning.

ability to minimize deviations from the operating point is affected.

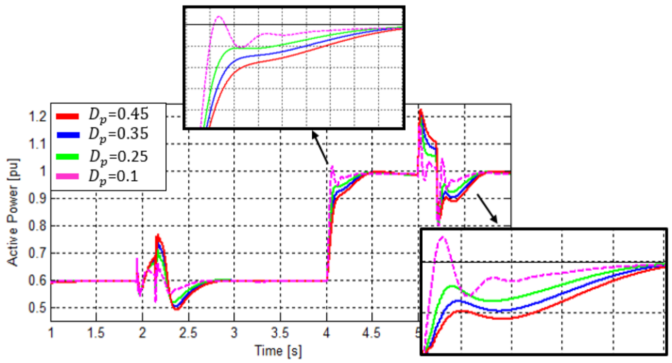

Figure 7. Active Power response for variations in governing system tuning

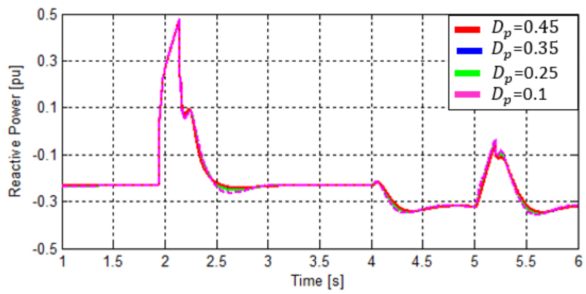

Figure 8. Reactive Power response for variations in governing system tuning.

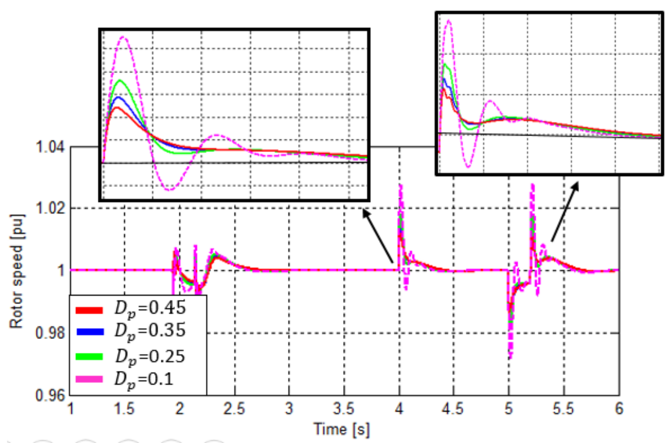

Figure 9. Rotor speed ω response for variations in governing system tuning.

Also, Fig 12 demonstrate that when a control system is at properly tuned, the efficiency is maximized and energy costs are minimized. Note that when the system is detuned, the control loop reaches the terminal voltage reference at the cost of additional reactive power supply.

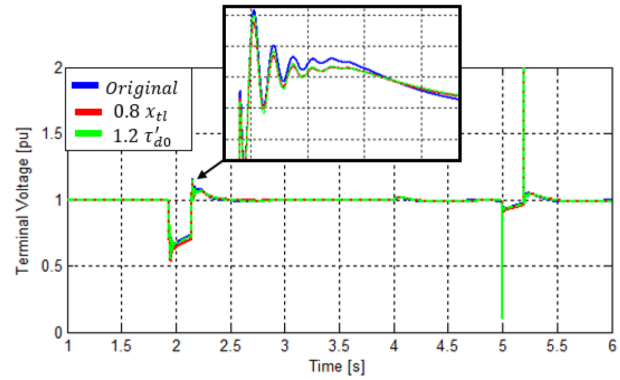

Figure 10. Terminal voltage for variations in excitation system tuning.

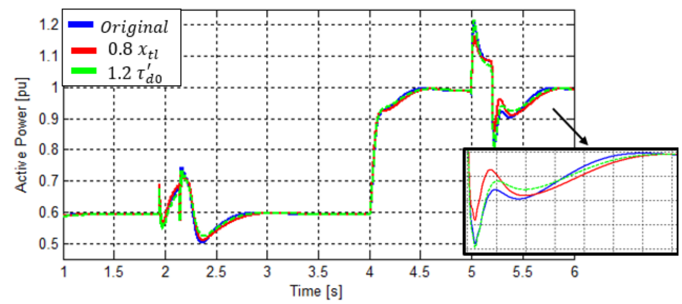

Figure 11. Active Power for variations in excitation system tuning.

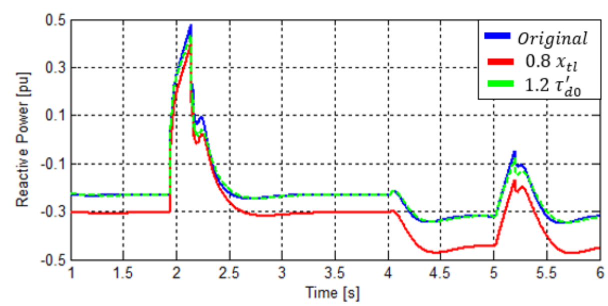

Figure 12. Reactive Power for variations in excitation system tuning.

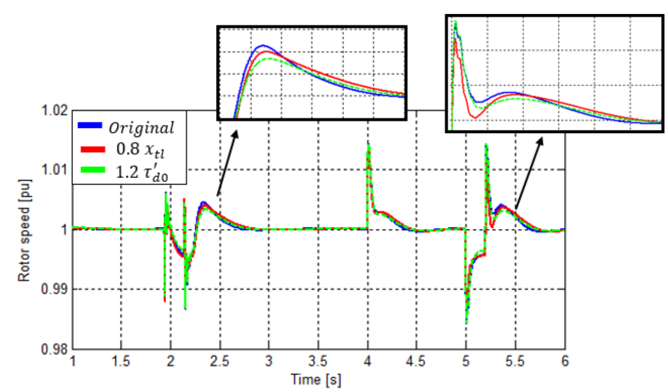

Figure 13. Rotor speed ω response for variations in excitation system tuning.

Finally, Fig. 14 presents a comparison between simulation results of a VSG with a similar synchronous machine under the same disturbances [12]. These results indicate that VSG and SM behavior are equivalent and the inverter can be controlled as a synchronous generator.

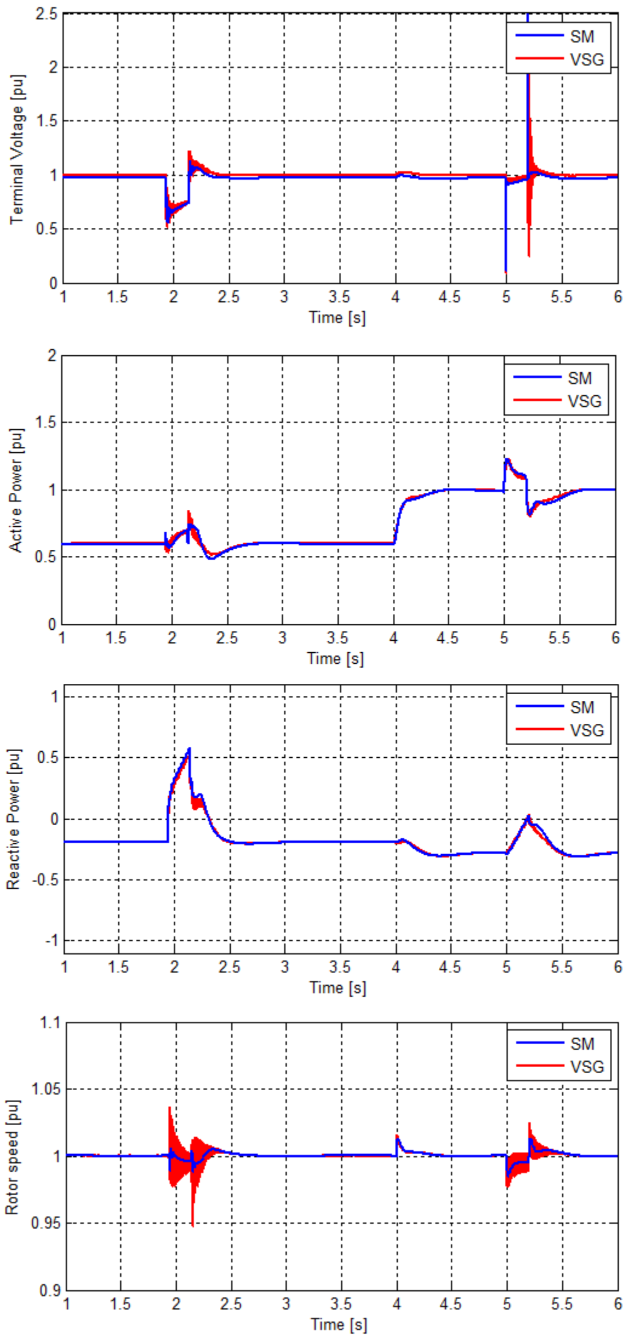

Figure 14. Comparison of simulation results of a VSG with an equivalent synchronous machine

V. Conclusion

This paper presents a VSG implementation and the procedures for tuning its speed and voltage controllers. A comparison of simulation results between the parameters obtained from the proposed methodology with respect to them without a proper control design, or when machine's data changes, has been performed. It has been demonstrated that performance characteristics such as settling time and oscillation are improved by the control tuning methodology. In addition, the validity of the presented VSG was obtained comparing simulation of a VSG with an equivalent SM, which indicates that a DG can emulate the SM behavior using a proper control mechanism.

References

[1]. Salvatore D'Arco and Jon Are Suul, "Virtual synchronous machines—Classification of implementations and analysis of equivalence to droop controllers for microgrids." in *PowerTech (POWERTECH), 2013 IEEE Grenoble*, 2013.

[2]. Yong Chen, R. Hesse, D. Turschner and H. P. Beck. "Improving the grid power quality using virtual synchronous machines." in *Power engineering, energy and electrical drives (POWERENG), 2011 international conference on*, 2011.

[3]. Salvatore D'Arco, Jon Are Suul and Olav B. Fosso. "Small-signal modelling and parametric sensitivity of a Virtual Synchronous Machine." in *Power Systems Computation Conference (PSCC), 2014*. IEEE, 2014.

[4]. P. Kundur. *Power system stability and control*, vol. 7, Eds. N. J. Balu, & M. G. Lauby. New York: McGraw-hill, 1994.

[5]. J. Machowski, J. Bialek and J. Bumby. *Power system dynamics: stability and control*. Ed. John Wiley & Sons, 2011.

[6]. C. E. Ugalde Loo, L. Vanfretti, E. Liceaga-Castro and E. Acha. “Synchronous generators modeling and control using the framework of individual channel analysis and design: part 1”, in *International Journal of Emerging Electric Power Systems*, vol. 8, n. 5, 2007.

[7]. *IEEE recommended practice for excitation system models for power system stability studies,* IEEE Std 421.5-1992, 1992.

[8]. R. C. Dorf and R. H. Bishop, *Modern control systems*,1998.

[9]. R. Teodorescu, F. Blaabjerg, M. Liserre and A. Dell'Aquila, “A stable three-phase LCL-filter based active rectifier without damping.” in *Industry Applications Conference, 2003. 38th IAS Annual Meeting*, vol. 3, pp. 1552-1557, October 2003.

[10]. Chang-Hua Zhang, et al. “An improved synchronverter model and its dynamic behaviour comparison with synchronous generator.” in *Renewable Power Generation Conference (RPG 2013), 2nd IET*. IET, 2013.

[11]. Y. Chen, R. Hesse, D. Turschner and H. P. Beck, “Comparison of methods for implementing virtual synchronous machine on inverters” in *International Conference on Renewable Energies and Power Quality-ICREPQ'12.*, 2012.

[12]. D. Carletti, J. F. Fardin and L. F. Encarnação, “Desenvolvimento de um Gerador Síncrono Virtual”, in *IEEE/ IAS International Conference on Industry Applications*, 2014.